



LAWRENCE  
LIVERMORE  
NATIONAL  
LABORATORY

# Phase diagram of Mo at high pressure and temperature

M. Ross

October 10, 2008

## **Disclaimer**

---

This document was prepared as an account of work sponsored by an agency of the United States government. Neither the United States government nor Lawrence Livermore National Security, LLC, nor any of their employees makes any warranty, expressed or implied, or assumes any legal liability or responsibility for the accuracy, completeness, or usefulness of any information, apparatus, product, or process disclosed, or represents that its use would not infringe privately owned rights. Reference herein to any specific commercial product, process, or service by trade name, trademark, manufacturer, or otherwise does not necessarily constitute or imply its endorsement, recommendation, or favoring by the United States government or Lawrence Livermore National Security, LLC. The views and opinions of authors expressed herein do not necessarily state or reflect those of the United States government or Lawrence Livermore National Security, LLC, and shall not be used for advertising or product endorsement purposes.

This work performed under the auspices of the U.S. Department of Energy by Lawrence Livermore National Laboratory under Contract DE-AC52-07NA27344.

10-01-08

## Phase diagram of Mo at high pressure and temperature

Marvin Ross\*

*Lawrence Livermore National Laboratory,  
University of California, Livermore, California 94551, USA*

We report values of the Poisson Ratios for shock compressed Mo, calculated from the sound speed measurements, which provide evidence that the 210 GPa ( $\sim 4100\text{K}$ ) transition cannot be a bcc-hcp transition, as originally proposed. Instead, we find the transition is from the bcc to a noncrystalline phase. For pressures above 210 GPa, the Poisson Ratio increases steadily with increasing temperature, approaching the liquid value of 0.5 at 390 GPa ( $\sim 10,000\text{K}$ ), suggesting the presence of a noncrystalline solid-liquid mixture. Free energy model calculations were used to show that the low melting slope of Mo, and the phase diagram, can be explained by the presence of local liquid structures. A new phase diagram is proposed for Mo that is constrained by the experimental evidence.

\* Correspondence: E:mail, [marvinross@earthlink.net](mailto:marvinross@earthlink.net)

PACS numbers: 61.25. Mv, 62.50.+p, 64.70.Dv, 64.70.Md

### I. Introduction

The phase diagram of molybdenum has become a controversial topic as the result of conflicting interpretations of shockwave melting measurements[1], laser heated Diamond-anvil-cell(DAC)[2-4] melting, and theoretical calculations[5-7]. The relevant data for Mo, taken from the above references, are plotted in figure 1. Chronologically, the narrative begins with shock experiments for Mo, made in 1989 by Hixson et al.[1], in which two discontinuities in the longitudinal sound speed were detected. One discontinuity is near 210 GPa ( $\sim 4100\text{K}$ ), and a second near 390 GPa ( $\sim 10,000\text{K}$ ). The first discontinuity has been interpreted as a bcc-hcp transition, and the second as hcp melting. While the pressures are measured, temperatures are calculated due to experimental limitations. Since the calculated temperatures vary with the theoretical

models, for consistency we employ the temperatures first reported by Hixson et al,[1]. Subsequently, the Mo melting curve was measured statically in a DAC to 90 GPa (3180 K), by heating the sample and observing a speckled motion in the liquid[2]. Clearly, an extrapolation of the DAC melting data plotted in figure 1 points toward the first shock discontinuity near 210 GPa, rather than the 390 GPa discontinuity. This suggests that the 210 GPa transition is an extension of the melting curve[3,4]. Since the low melting slope of Mo is at odds with the predictions of theoretical calculations and computer simulations, this has led to speculations that the DAC phase melting measurements are actually of a high temperature bcc to a close-packed(fcc or hcp) transition[5-7].

The purpose of this paper is to provide new information gained from the shock experiments that help to clarify the phase diagram. In section II, we report values of the Poisson Ratio calculated from the sound speed shock data[1] that lead to the conclusions that a bcc-hcp transition cannot be present in the Mo phase diagram, and that the sequence of structures is more complicated than previously suspected. In section III, melting calculations made with a free energy model are reported that show the presence of local structures in the liquid will lead to the low melting slopes and explain many features of the phase diagram. The summary, section IV, includes a proposed phase diagram.

## II. Poisson Ratios and the Mo phase diagram.

The Poisson Ratio( $\nu$ ) is the ratio of strain in the lateral direction, relative to the strain in the longitudinal direction. It can be calculated from the longitudinal( $C_L$ ) and bulk( $C_B$ ) sound speeds measured in shock experiments[1] by using the expression,

$$C_L/C_B = [3(1-\nu)/(1+\nu)]^{1/2}.$$

In the present application, Poisson Ratios provide, a limited, but useful, criteria for examining structural changes in solids. For isotropic materials, such as ideal bcc and close-packed structures like hcp and fcc,  $\nu=0.25$ , and for liquids  $\nu=0.5$ . For Mo  $\nu = 0.31$ , and for Al  $\nu = 0.32$ . For most close-packed metals  $\nu$  is in the range 0.28 to 0.36. For the purpose of this study we refer to any phase of Mo with a value of  $\nu$  above this range, as

non-close-packed. Our use of this term necessarily includes phases such as glasses, amorphous solids, etc. that may be present, but are beyond our ability to designate.

In order to acquire some guidance in interpreting the Mo data, we first consider the sound speed measurements of Shaner et al.[9] that lead to the detecting shock melting of Al. Al melting has been measured in a DAC[10], and it is understood to be a transition directly from an fcc solid to a pure atomic-like liquid[11]. Plotted in figure 2, are the sound speed measurements of shock compressed Al and Mo[1] versus the Hugoniot pressure. The sound speeds for fcc Al, increase linearly with pressure up to 120 GPa and then show a discontinuous drop to the liquid caused by the loss of shear strength in the solid. A data point has been taken in the mixed phase region at 145 GPa is indicative of a mixed solid-liquid phase. The Poisson Ratios calculated for Al are plotted in figure 3. In the fcc phase, they show a small increase in the Ratio from  $\nu=0.32$  at  $P=0$ , to  $\nu=0.34$  near 120 GPa. This is followed by a discontinuous jump (melting) to the liquid value of  $\nu=0.5$ . The singular experimental point at 140 GPa, and  $\nu=0.46$ , lies in the mixed phase region.

In the case of Mo, an interpretation of the sound speed data is problematical. The values of  $\nu$  obtained from the reported Mo sound speeds[1] are plotted in figure 4. Noteworthy is the absence of shock measurements below 150 GPa. A similar plot can be constructed for Ta[9]. Following the example of Al we assume the  $P=0$  GPa bcc value of  $\nu=0.31$ , remains a constant up to 90 GPa, the highest pressure at which Mo DAC melting measurements were made. The value of  $\nu$  then increases to  $\nu=0.42$ , near 150 GPa, which is the lowest pressure at which shock measurements were made. This means that none of the shock measurements made for Mo were in the bcc phase. Clearly then, there must be a bcc-to non-crystalline transition starting at some pressure between 90 to 150 GPa (~3000K). This would place the transition in agreement with a linear extrapolation of the DAC melting curve.

At pressures above 150 GPa, the values of  $\nu$  decrease sharply to 210 GPa, and rise again to 220 GPa. This is the discontinuity reported as the 210 GPa transition, and it is not directly from the bcc phase, but it is from a structure in the intermediate pressure range from 150 GPa and 210 GPa. Hixson et al.[1] had noted, that at 210 GPa the Poisson

ratio of 0.4 was considerably higher than the normal density value. For pressures above 210 GPa the value of  $\nu$  rises steadily to  $\nu=0.44$  at 380 GPa, where it melts to the liquid value of  $\nu=0.5$  at 390 GPa. The nearly linear increase in the Poisson Ratio above 210 GPa indicates a continuous loss of shear strength. This loss is consistent with a solid-liquid mixture in which the liquid fraction is increasing as it approaches the pure liquid. While the Poisson Ratios do not provide specific determinations of the atomic structures they do eliminate the possibility of a bcc-hcp transition at 210 GPa.

### III. Mo melting and local liquid structures.

The key to unlocking the Mo phase diagram is linked to understanding the physics underlying the origin of the low melting slope. Low melting slopes have now been found in all seven of the early transition metals studied[3], Ta, W, Cr, Ti, V, Y, indicating that the measurements for Mo are not unique, but are characteristic of this class of metals. The origin of these low melting temperatures has been attributed to the presence in the liquid of tetrahedral and icosahedral structures with short range order(ISRO). Evidence for the presence of these local structures in the liquid is supported by an extensive body of experimental and theoretical investigations[12-20]. Since ISROs are denser than the atomic liquids, compression favors an increase in their concentration, and communal entropy, thereby lowering the free energy of the liquid and the melting temperature.

At the atomic level, the origin of these local structures has been attributed to Peierles/Jahn-Teller(P/JT) distortions[21,22] of the *d*-electron bonding leading to the presence in the liquid of energetically preferred local structures with poly-tetrahedral and five-fold icosahedral short range order(ISRO)[3,4]. In the case of Mo, P/JT distortions are optimal. With nearly half-filled *d*-bands, the distortion lowers the energy of the occupied bonding states while the unoccupied anti-bonding states are raised in energy. Frank[23] was the first to suggest that local structures in liquid metals based on the packing of five-fold symmetric icosahedral units could explain supercooling. By employing the free energy model described below, we are in effect extending Frank's proposal to the idea, that local structures in transition metals can be pressure stabilized and be responsible for the low melting slopes found in transition metals.

While a rigorous study is beyond the scope of this report, a considerable degree of insight into the role played by local structures can be gained by employing a free energy model. A version of this model was employed previously[24,25]. We examine two cases. First is by a calculation in which local structures are absent, and a second in which the free energy contribution by the local structures is approximated. For the first case, we write the excess Helmholtz free energy for a system of solid and liquid atoms interacting by inverse-power repulsive potentials,  $\phi(r)=B/r^n$ , as,

$$F_{ex}^s = U_M + F_{th-inv}^s, \quad (3)$$

$$F_{ex}^l = U_M + F_{th-inv}^l.$$

In each expression, the first term is the Madelung energy ( $U_M$ ) of the solid and the second is of the thermal free energy of atomic motion in the solid and liquid respectively. The thermodynamic properties of the inverse power potential has been studied extensively by computer simulations, and the thermal free energy terms in (1) have been fitted to analytic expressions of the free energy [25]. Although the same  $U_M$  is used to represent the solid and liquid Madelung energy, the thermal contributions to the liquid free energy are determined from a fit to the total excess free energy, in effect correcting for the Madelung term. This is a reasonable approximation for transition metals, in which the volume changes of melting are typically 1-2 %.

A useful simplification for real systems is to replace the Madelung energy,  $U_M$ , by  $U_{Lat}$  the lattice energy determined from a Birch-Murnaghan fit to the experimental room temperature isotherm [26], corrected to T=0 K. The excess Helmholtz free energy can now expressed written as,

$$F_{ex}^s = U_{Lat} + F_{th-inv}^s. \quad (4)$$

$$F_{ex}^l = U_{Lat} + F_{th-inv}^l.$$

The model has the attractive feature that it reproduces the room temperature solid isotherm, and provides a thermodynamically consistent set of solid and liquid free energy functions. Melting is determined by matching free energies of the two phases.

As it stands, the model requires two adjustable parameters,  $B$  and  $n$ , in the potential. As in the bcc-hcp case we chose  $n=6$ , and  $B= 400 \text{ eV-cm}^6$ , values that had been determined by fitting the model predictions to the experimental Mo Hugoniot[23]. Using these parameters two sets of melting calculations were made. In one set, using equations (4), atoms in the bcc solid melt to an atomic liquid. In the second set, terms were added to the liquid free energy in order to account for the influence local structures. In this case, the free energy of the liquid is modified to,

$$F_{ex}^l = U_{Lat} + F_{th-inv}^l + xU_{cl}^l + kT[x \ln x + (1-x) \ln(1-x)]. \quad (5)$$

The added terms are,  $U_{cl}$  the binding energy of a local structure, and the communal entropy of liquid-cluster mixing. Since  $U_{cl}$  is unknown, and to avoid adding poorly known parameters we set  $U_{cl}=0$ . The parameter  $x$  is defined here as the volume fraction of local structures the melt,  $x=V_{st}/V$ , where  $V_{st}$  is the effective total volume of local structures in a volume,  $V$ . The volume fraction,  $x$ , is used here as a parameter to fit the DAC melting measurements and the 210 GPa shock discontinuity. By adjusting value of  $x$  to fit the measurements it implicitly includes contributions from the omitted  $U_{cl}$  and geometric frustration that is not a thermodynamic driver, but does act to inhibit long-ranged order and crystalline formation. The present model is not predictive, but its usefulness is that it is transparent, and connects the DAC, and shock measurements to the phase diagram in a thermodynamically consistent, and physically realistic manner.

Figure 5 shows the DAC melting measurements, the shock melting points, and calculations made with the present model of melting, without local structures and with local structures fitted to the DAC and 210 GPa shock discontinuity. The melting curve calculated by omitting local structures is in very good agreement with the computer simulations of Belonoshko et al.[5], in figure 1. The fraction of local structures required to fit the melting measurements are plotted in figure 6. The fraction rises steadily to a maximum of  $x=0.5$ , at 150 GPa(3500 K) and remains constant. We interpret the 150 GPa melting as being roughly the pressure at which the fraction of local liquid structures has become sufficiently large as to create a solid-liquid mixed phase.

#### IV Summary and proposed phase diagram

In order to summarize our results most directly, while satisfying the constraints imposed by the Poisson Ratios, we propose the phase diagram described in figure 7. The bcc phase is extended at 3000 K to 150 GPa, the pressure at which the Poisson Ratios pointed to a transition from bcc to a new noncrystalline phase, possibly A15. The melting curve extends to the 210 GPa shock discontinuity. Above 150 GPa the melt is a solid-liquid mixture bounded roughly by a transition region extending from 150 GPa(4100K) to 390 GPa(10,000K). The solids are likely A15 polytetrahedral structures, that are known to compete favorably with bcc, for the neighboring metals Mo, Nb, Ta

and W[15]. The predictions in this report, particularly of the absence of a bcc-hcp transition, can be verified by new shock measurements of the sound speeds between about 100 and 200 GPa. The experimental facilities exist and the expertise is available.

*Acknowledgements:* The work by MR was performed under the auspices of the U.S. Department of Energy, by the Lawrence Livermore National Laboratory under Contract DE-AC52-07NA27344. We wish to thank Drs. D. Errandonea, R. Boehler, and D. Santamaria-Perez for useful discussions. Thanks also to the Max-Planck-Institute für Chemie at Mainz, Germany for its hospitality.

## References

- 1) R.A. Hixson, D.A. Boness, J.W. Shaner and J.A. Moriarty, *Phys. Rev. Lett.* **62**, 637 (1989).
- 2) D. Errandonea, B. Schwager, R. Ditz, R. Boehler and M. Ross, *Phys. Rev. B* **63**, 132104 (2001).
- 3) M. Ross, R. Boehler and D. Errandonea, *Phys. Rev. B* **76**, 184117 (2007).
- 4) M. Ross, D. Errandonea and R. Boehler, *Phys. Rev. B* **76**, 184118 (2007).
- 5) A.B. Belonoshko, et al. *Phys. Rev. Lett.* **100**, 135701 (2008).
- 6) C. Cazorla, M.J. Gillan, S. Taioli, and D. Alfè, *J. Chem. Phys.*, **126**, 194502 (2007).  
C. Cazorla, D. Alfè and M.J. Gillan, *Phys. Rev. Lett.* **101**, 049601 (2008).
- 7) A.S. Mikhaylushkin et al. *Phys. Rev. Lett.* **101**, 049602 (2008).
- 8) J.A. Moriarty, *Phys. Rev. B* **45**, 2004 (1992).
- 9) J. Shaner, J.M. Brown and R.G. McQueen, *Mater. Res. Soc. Symp. Proc.* **22**, 137 (1984).
- 10) R. Boehler and M. Ross, *Earth Planet. Sci. Lett.* **153**, 227 (1997).
- 11) J. A. Moriarty, D.A. Young, and M. Ross, *Phys. Rev. B.* **30**, 578 (1984).
- 12) T. Schenk, D. Holland-Moritz, V. Simonet, R. Bellissent, and D.M. Herlach, *Phys. Rev. Lett.* **89**, 075507 (2002).
- 13) G.W. Lee, A.K. Gangopadhyay, K.F. Kelton, R.W. Hyers, T.J. Rathz, J.R. Rogers, and D.S. Robinson, *Phys. Rev. Lett.* **93**, 1982 (2004).
- 14) T.H. Kim and K.F. Kelton, *J.Chem.Phys.* **126**, 054513 (2007).
- 15) C. Berne, A. Pasturel, M. Sluiter, and B. Vinet, *Phys. Rev. Lett.* **83**, 1621 (1999).
- 16) N. Jakse and A. Pasturel, *J.Chem.Phys.* **120**, 6124 (2004).
- 17) N. Jakse and A. Pasturel, *J.Chem.Phys.* **123**, 244512 (2004).
- 18) N. Jakse and A. Pasturel, *Phys. Rev. Lett.* **91**, 195501 (2003).
- 19) N. Jakse, O. Le Bacq, and A. Pasturel, *Phys. Rev. B.* **70**, 174203 (2004).
- 20) B. Lee and G.W. Lee, *J.Chem.Phys.* **129**, 024711 (2008).
- 21) R.E. Peierls, *Quantum Theory of Solids*, Oxford (1955)
- 22) H.A. Jahn and E. Teller, *Proc. Soc. London, Ser. A* **161**, 220 (1937).
- 23) F.C. Frank, *Proc. R. Soc. London, Ser. A* **215**, 43 (1952).
- 24) M. Ross, L.H. Yang, and R. Boehler, *Phys. Rev. B* **70**, 184112 (2004).
- 25) D.H.E. Dubin, and H. DeWitt, *Phys. Rev. B* **49**, 3043 (1994).

26) A.L. Ruoff, H. Xia , H. Luo and Y. K. Vohra, Rev. Sci. Instrum. **61**, 3830(1990).

Figure captions

Fig. 1 Mo melting and shock transition data. DAC melting, open circles[4] extended to 210 GPa(small dashed line). Shock transitions(crosses)[1] and calculated Hugoniot(solid curve)[8]. Calculated melting curves of[5](dash-dotted), and of[6](long dashes).

Fig. 2 Longitudinal and bulk sound velocities for Al[9] and Mo[1].

Fig. 3 Poisson Ratios for Al, versus pressure.

Fig. 4 Poisson Ratios for Mo, versus pressure.

Fig. 5 Calculated model melting curves. DAC open circles[3,4]. Melting curves omitting local structures(small dashed curve), and including local structures by fitting to measurements(dash-dotted). Shock transitions(crosses)[1].

Fig. 6 Calculated volume fractions of local structures in the melt, versus pressure.

Fig. 7 A proposed Mo phase diagram. Described in text. DAC melting(open circles)[4]. Shock transitions (crosses)[1]. The long dashed line is an extension of the DAC melting curve. The small dashed curve is a bcc to non-close-packed solid phase line. The small open circle(o) at 150 GPa(3000K) is a predicted transition from the bcc to a non-crystalline solid. The dashed-dotted vertical line defines roughly a predicted liquid melt to a solid liquid phase line.

Figure 1

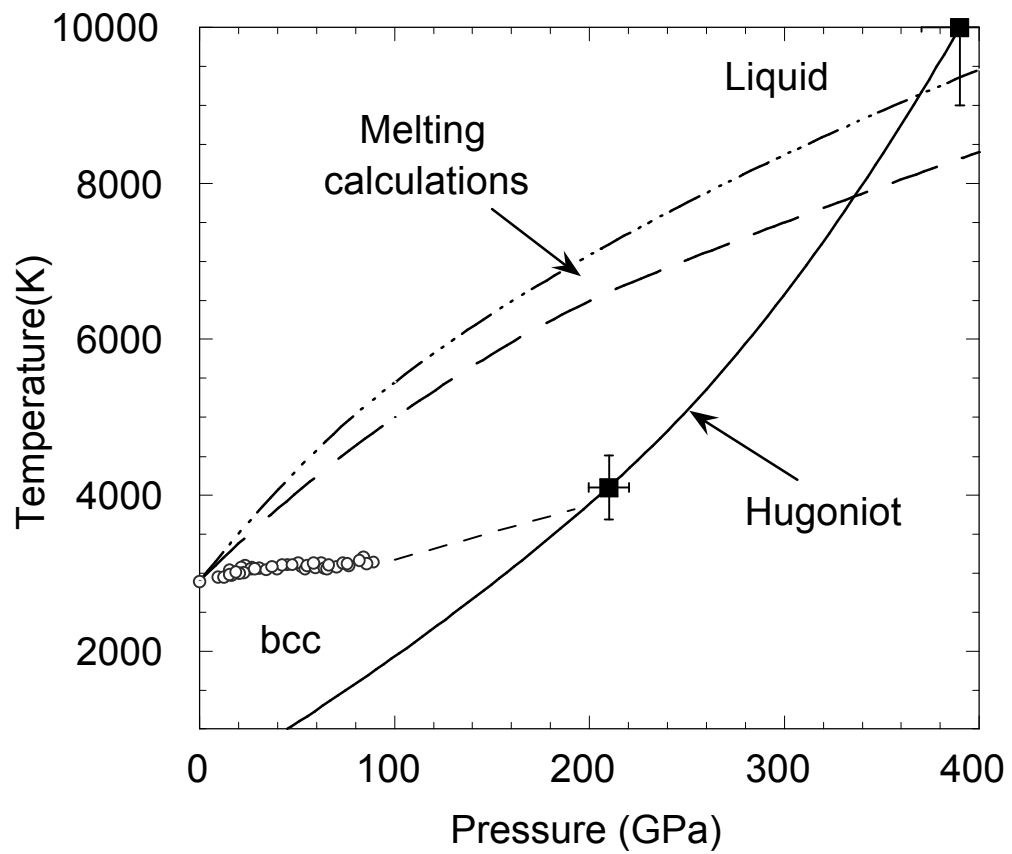


Figure 2

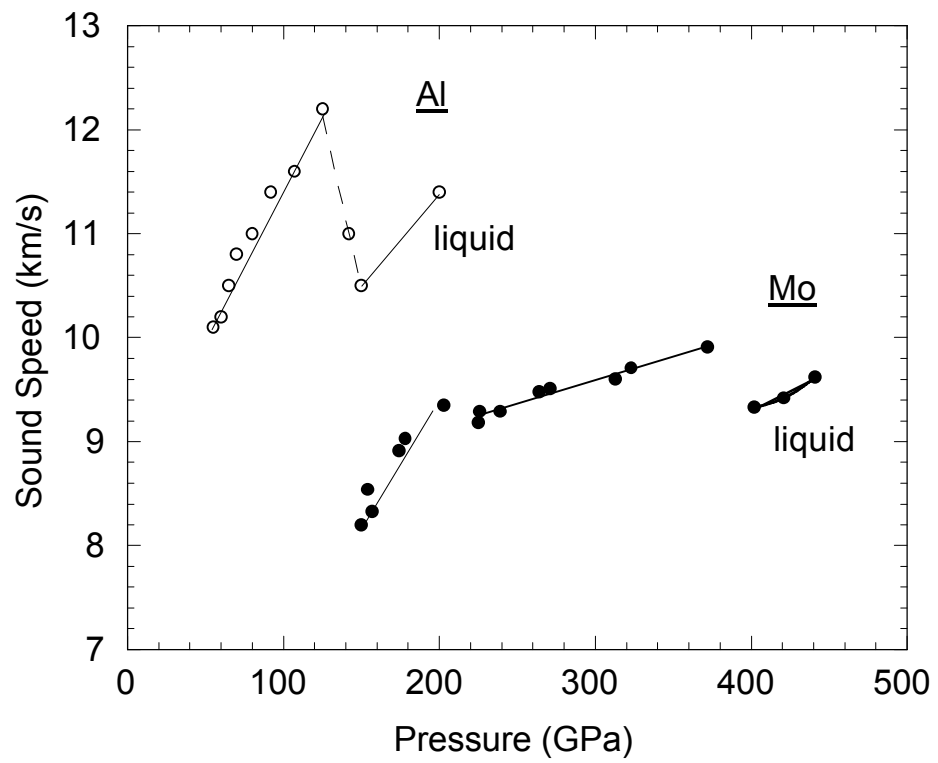


Figure 3

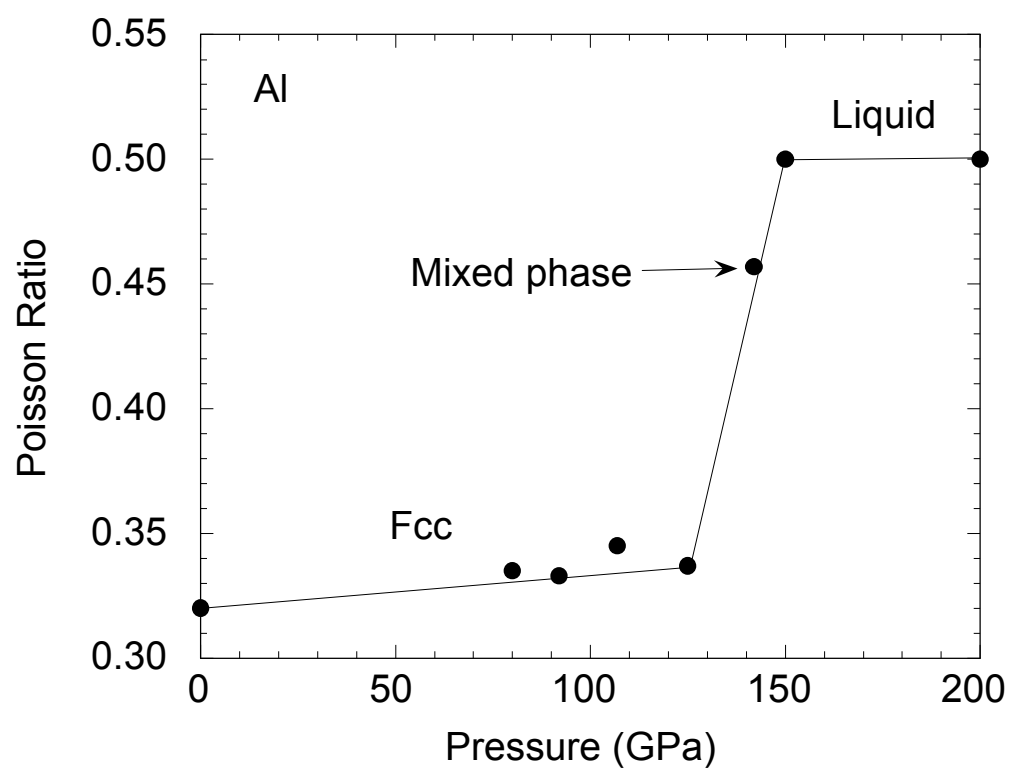


Figure 4

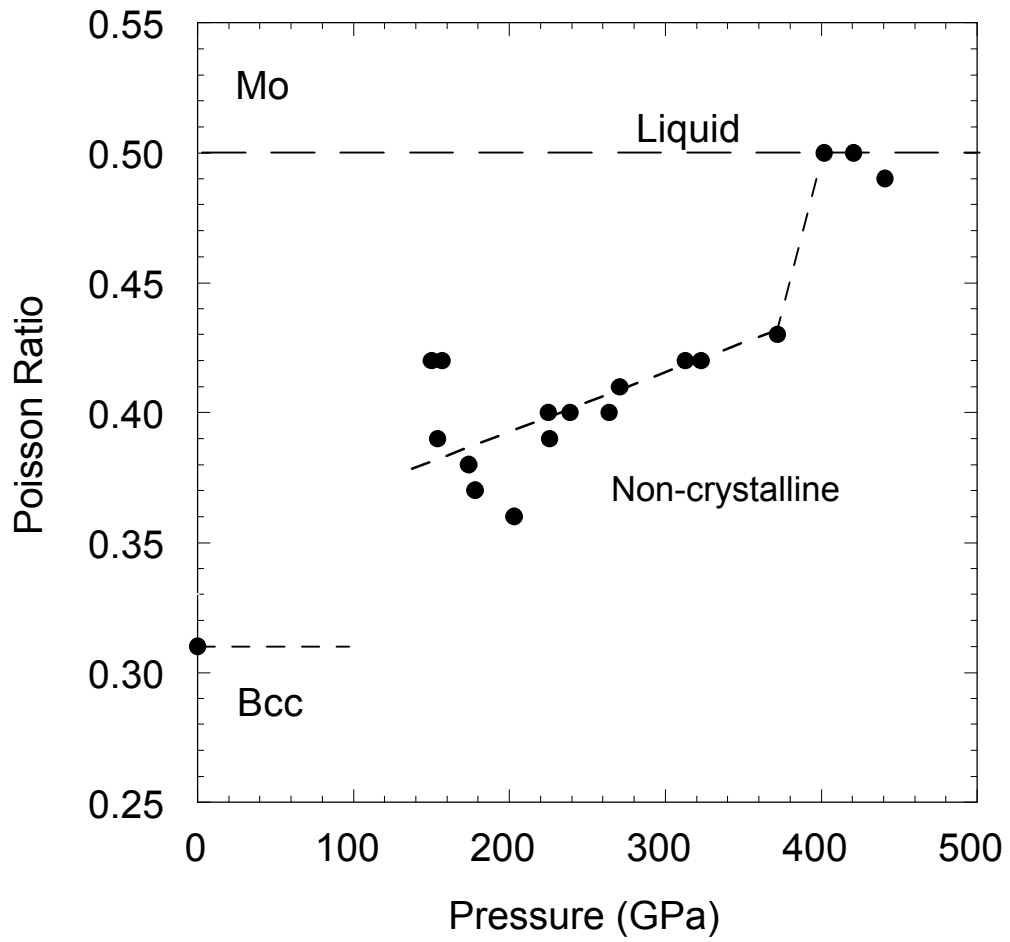


Figure 5

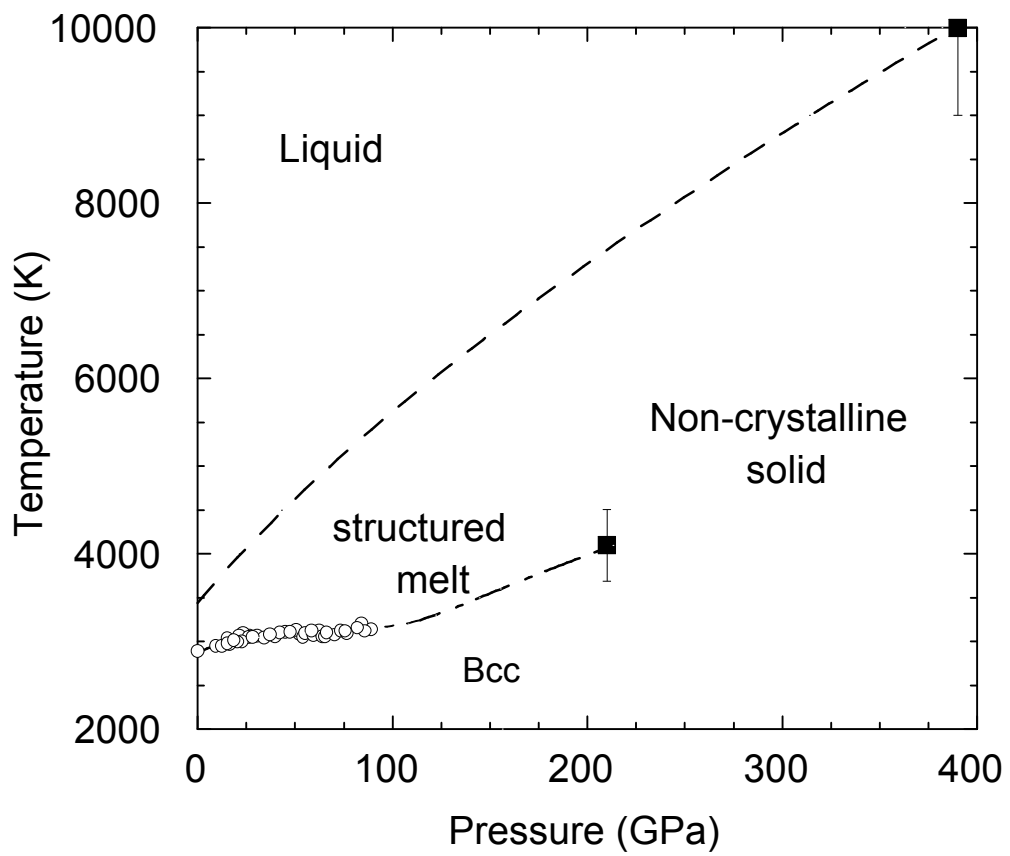


Figure 6

